Parallel formation of opposing memories tunes online and pre-emptive control of learned behavior in eyeblink conditioning

Authors: Ryota Iwase[1], Shin-ya Kawaguchi[1, *]

[1] Department of Biophysics, Graduate School of Science, Kyoto University; Kyoto, 606-8502, Japan.

*Corresponding author, e-mail: kawaguchi@nb.biophys.kyoto-u.ac.jp

Abstract

Animals change their behavior and adapt to the environments through associating patterns of sensory experiences, making memories to acquire and/or cease actions. However, it remains to be clarified how distinct memories are formed and interact in response to altered sensory inputs. Here we studied this issue using contrasting paradigms for eyeblink conditioning in mice, and demonstrated a fundamental mechanism of memory counteraction to fine-tune the adaptive change of animal behavior. Excessive neutral sensory stimulation intermingled with the paired presentation of two sensory stimuli did not disturb the acquisition of conditioned responses, but gradually suppressed the occurrence of learned behavior during individual daily sessions. Modeling of acquisition and extinction processes, coupled with experimental validation of a model prediction, unveiled independent and parallel formation of long-term opposing memories for execution of eyeblink and its suppression irrespective of the temporal order: the memory to suppress the conditioned response can, surprisingly, be formed even before its acquisition. Consequently, the negative memory formed either online or pre-emptively calibrates the acquired behavior, optimizing motor performance reflecting both positive and negative sensory histories.

Introduction

Animals adapt to changing environments by learning from experience, whose richness has been thought to affect the efficiency of adaptive behavior (Grant & Shipper, 1952; Thomas & Wagner, 1964). Notably, animals need to adaptively change the behavior even through a survival-related critical, but rare, experience in the natural environment. Such an acquired behavior can also be modulated by the later experience as evident in the memory extinction through repetitive activation of one sensory pathway to unrelate it from another sensory experience (Robleto et al., 2004; Delamater, 2004; Bouton, 2004; Rescorla, 2004; Thanellou & Green, 2011). Critically, it remains enigmatic how the brain reconciles conflicting sensory experiences such as the coincidental and independent occurrences of stimuli to calibrate behavioral outputs. Specifically, whether excitatory and inhibitory memories develop through a common associative process or emerge as independent, parallel traces remains a fundamental question in systems neuroscience. Here we studied this issue using classical eyeblink conditioning in mice, which has been extensively studied for a century to assess learning ability and the underlying neural circuits in a variety of species including humans (Cason, 1922; Christian & Thompson, 2003; Heiney et al., 2014).

Repeated presentation of conditioned stimulus (CS; e.g., tone or light) coupled with eyelid reflex-inducing unconditioned stimulus (US; e.g., air puff to cornea) typically at a high probability (~90%) makes animals learn to blink in response to the initially neutral CS. Such acquired responses through training are called conditioned responses (CRs). Previous studies demonstrated that the even halved pairing of sensory inputs is effective to establish CRs (Thomas & Wagner, 1964; Leonard & Theios, 1967; Gormezano & Coleman, 1975; Buchanan et al., 1997; Kehoe et al., 2008), but it remains unclear how the learning is affected by mingling of frequent neutral sensory stimulation which possibly leads to extinction. Increasing neutral CS-alone has

been associated with memory erasure/extinction, and latent inhibition, the lowered efficiency of subsequent memory acquisition (Lubow & Moore, 1959; Schmajul et al., 1994; Nicholson & Freeman, 2002), although these have been regarded as distinct phenomena. Recent elegant experiments in diverse species from fly to mammals have suggested that memory extinction relies on the experience-dependent formation of another memory to counteract the original memory encoding an action (Kim et al., 2020; Felsenberg et al., 2018). However, the nature and the way of this suppressing memory to counteract the learned behavior is totally unclear in terms of cellular and circuit-level of plasticity in the mammalian cerebellar circuits. In this study, by systematically changing the enrichment of sensory pairings, we quantitatively investigated the acquisition and extinction of associative eyeblink learning. Counter-intuitively, we found that a much less or lower density of associative experience is not only sufficient but substantially more efficient per trial for the establishment of well-timed eyelid closure. Our detailed analysis of experimental data yielded a computational model demonstrating that learned behavior is established by the parallel formation of two opposing long-term memories: one for execution of eyeblink and the other for suppression. The model predicted that the suppressive memory can be pre-emptively established even before acquisition, which was experimentally validated, leading to the conclusion that the adaptive behavior is the outcome of counteraction between two opposing long-term memories.

Results

Eyeblink conditioning with limited paired sensory stimuli

To obtain insights into the formation and interaction of memories controlling animals' behavior in response to distinct patterns of sensory experience, we first examined the effect of altered ratio

of two sensory stimuli: tone (290 ms) and air puff (to a cornea, 40 ms) as CS and US, respectively (Fig. 1A, B). Mice were head-fixed on a treadmill during experiments (Fig. 1C) and their eyelid movements were recorded with a monochrome camera, and the eyelid closure level was quantitated by calculating the area size of an eyeball (Fig. 1D; Heiney et al., 2014; for details see Materials & Methods). Air puff delivered via a glass tube or a needle elicited quick eyeblink responses (unconditioned responses, URs), whereas tone did not affect the eyelid (Fig. 1D, before). For association of two sensory events in mice, combined and co-terminating sensory inputs of CS and US in time series are provided typically at a high ratio: 90 paired & 10 CS-alone trials ($90\%_{CS\text{-}US}$, Fig. 1A). In line with previous studies (Heiney et al., 2014; Fiocchi et al., 2022), CRs were evident in ~10 out of 100 trials on average even on the 1st day, gradually becoming frequent (~ 50%) and larger by ~ day4, which remained nearly constant till day10 (Fig. 1E, F), although showing variable time courses in individual mice (Fig. S1A). On the other hand, unexpectedly, even when the pairing of CS and US was lowered to 10% (i.e., 10 paired & 90 CS-alone per day: $10\%_{CS\text{-}US}$, Fig. 1A), mice acquired CRs during 10 days training (Fig. 1E, middle) although hitting a plateau around 30% on day6 (Fig. 1F). Thus, even 9 times less association of CS and US inputs succeeded in the establishment of eyeblink conditioning, while the final probability for the CR triggering was apparently lower with a tiny delay in reaching equilibrium (Thomas & Wagner, 1964; Leonard & Theios, 1967; Gormezano & Coleman, 1975; Buchanan et al., 1997; Kehoe et al., 1983). Notably, the number of paired trials required for CR acquisition was significantly lower in the sparse pairing groups, indicating that frequent CS-alone trials do not interfere with, but rather highlight, an underlying high-efficiency learning mechanism.

Two factors could underly the lower percentage of CRs (%CR) in the $10\%_{CS\text{-}US}$ group: insufficient paired sensory experience or excessive presentation of unpaired tone. To discriminate these, another paradigm “11 trials” was examined (10 paired & 1 CS-alone per day), where the

limited paired sensory experience was the same as the $10\%_{CS\text{-}US}$, but the excessive tone-alone stimulation was omitted (Fig. 1A, B). As shown in Fig. 1E, F and S1A, even the daily 10 CS-US pairings effectively established CRs reaching ~50% in 6 days training, similarly to the daily 100 trials in the $90\%_{CS\text{-}US}$, although slight delay in reaching plateau. Success rate of learning in individual mice in three groups was similar, although slightly low in the $10\%_{CS\text{-}US}$ group (Fig. S1B). These results altogether indicate that small number of paired sensory stimuli (10 pairings per day) are sufficient for the CR acquisition, while additional massive tone-alone events only lowered final probability of learned behavior. Notably, considering that the probability of air puff was just 10% out of total tone presentations in the $10\%_{CS\text{-}US}$, the final %CR as ~30% could be rather regarded as exaggerated occurrence of acquired behavior.

While the 10% CS-US group exhibited a slower increase in daily %CR compared to the 90% group, a strikingly different picture emerged when the data were normalized by the number of paired trials. When the averaged %CR was plotted as a function of total CS-US pairings, surprisingly, the $10\%_{CS\text{-}US}$ and the 11 trials groups exhibited very quick establishment of CRs compared to the conventional $90\%_{CS\text{-}US}$ group (Fig. 1G). The courses of increase in %CR were fitted by the following equation:

$$\%CR = P_{max} * \frac{1}{1 + (\frac{L_{50}}{N_{paired}})^n}$$

, where P_{max}, L_{50}, n, and N_{paired} represent the maximal %CR, the number of paired stimuli for the half-maximal learning, the steepness of learning, and the number of given paired trials. In sharp contrast to the similar n in three groups, L_{50} reflecting the number of sensory inputs needed for learning was ~6 folds higher in the $90\%_{CS\text{-}US}$ group. Thus, the sparse pairing protocol achieved superior learning efficiency, reaching the L_{50} with nearly six-fold fewer pairings, in contrast to previous findings in rabbits (Thomas & Wagner, 1964; Leonard & Theios, 1967; Gormezano &

121 Coleman, 1975). Step-by-step pattern of %CR increases were evident in the 90%$_{CS\text{-}US}$ group
122 during initial 4 days, implying some daily upper limit for learning such as a gradual attenuation
123 of its efficiency during repetitive training (Tait et al., 1983; Kehoe & White, 2002). Intriguingly,
124 the %CR in the 10%CS-US group was initially compatible at the beginning of each daily trials to
125 the 90%CS-US and the 11 trials groups, but selectively exhibited a gradual decline during daily
126 sessions (Fig. 1G, inset). Thus, tone-alone trials do not disturb the acquisition, but distract the
127 expression of learned CRs. Furthermore, taking into consideration that the total trial number is
128 identical in 10%- and 90% CS-US groups, the "within-session decline" of %CR evident only in
129 the 10% group implies a gradually emerging process to actively suppress the CR occurrence.
130 The acquired eyeblink responses were similarly sophisticated in timing and amplitude
131 although the averaged eyelid closures in the 10%$_{CS\text{-}US}$ group were apparently smaller because of
132 larger variability of peak timing (Fig. 2A-C). The CR amplitude grew up gradually during days
133 of training and showed faster saturation in the 10%$_{CS\text{-}US}$ and the 11 trials groups in relation to the
134 number of paired trials, while onset/peak timings got quickly optimized in all groups (Fig. S2A-
135 E) (Heiney et al., 2014; Kehoe et al., 2008; Fiocchi et al., 2022; Balsam et al., 2002; Ohyama &
136 Mauk, 2001; Kehoe et al., 2014). With a closer look, the 10%$_{CS\text{-}US}$ group occasionally exhibited
137 rapid and complete eyelid closure (RCEC), reaching 98% eyelid closure during 80-180 ms from
138 the tone onset, which looked similar to that of spontaneous eye blinking (Fig. S3A-C). As a result
139 of more RCEC occurrence, well-timed blinking relative to the timing of air puff, which was
140 regarded to be cerebellum-dependent CRs, was slightly rarer in the 10%$_{CS\text{-}US}$ group (Fig. S3D),
141 while total probability of eyeblink responses including CRs and RCEC was almost compatible in
142 three groups (Fig. S3E).
143
144 **Critical role of DCN in CR expression**

145 Deep cerebellar nuclei (DCN) plays an important role in expression of CRs in rabbits (Christian
146 & Thompson, 2003; McCormick & Thompson, 1984; Yeo et al., 1985) and mice (Heiney et al.,
147 2014; Sakamoto & Endo, 2008). To examine whether the CRs acquired with $10\%_{CS\text{-}US}$ also rely
148 on DCN, we pharmacologically inhibited neuronal activity by infusing muscimol, a selective
149 $GABA_A$ receptor agonist, to the anterior interpositus part of DCN through a cannula implanted in
150 the already CR-acquired mice (Fig. 3A). As shown in Fig. 3B, cannula position and estimated area
151 for diffusion of muscimol were similar in the two groups (90% and 10% CS-US pairing groups).
152 Muscimol administration (evaluated by at least 30 trials given before and after its infusion)
153 potently abolished the CR expression in both the 90% and 10% CS-US pairing groups, followed
154 by almost complete recovery on the next day (Fig. 3C). Averaged traces for eyelid closure
155 indicated marked abolishment of CRs by muscimol, but not by artificial cerebrospinal fluid
156 (aCSF), without affecting the URs upon air puff (Fig 3C-F). Taken these results together, it was
157 revealed that CR is expressed depending on the DCN activity irrespective of the altered
158 enrichment of paired sensory experience.

159 Scatter plots of averaged eyelid closure amplitude against %CR exhibited a tendency of
160 the $90\%_{CS\text{-}US}$ showing positive relation between them (Fig. S4A, left), which was preserved even
161 after the DCN inactivation. In contrast, the $10\%_{CS\text{-}US}$ group showed less correlation between %CR
162 and eyelid closure amplitude, sometimes exhibiting unaltered amplitude even after the DCN
163 inactivation (Fig. S4A, right). Furthermore, RCEC sometimes evident in the $10\%_{CS\text{-}US}$ group
164 tended to resist to the DCN inactivation (Fig. S4B). Thus, limited experience and disturbance by
165 lots of CS-alone inputs in the $10\%_{CS\text{-}US}$ group might be partly compensated by recruiting neural
166 circuits other than the cerebellar circuit for eliciting eyelid closure (Kaminer et al., 2011; Kaminer
167 et al., 2015; Bologna et al, 2024). Nevertheless, the similar impact of DCN inactivation on CR
168 execution, irrespective of altered enrichment of sensory pairings, indicates that the occurrence of

169 learned behavior is primarily governed by the DCN, probably with slight difference in experience-
170 dependent circuits modulation mainly in the cerebellum.
171
172 **Distinct extinction dynamics of CRs acquired with altered enrichment of sensory experience**
173 In order to evaluate the qualitative identity of CR-memories acquired by different patterns of
174 experience, we examined memory-extinction paradigm. Following 10 days of acquisition training,
175 100 tone-alone (i.e. 100 CS-alone) trials were daily applied for 4 days. CR occurrence gradually
176 decreased during the extinction session with clearly different kinetics according to the distinct
177 pattern of acquisition (Fig. 4A-C). Looking at gradual changes during daily sessions, %CR
178 substantially recovered at the beginning of individual daily sessions (Fig. 4B), known as
179 spontaneous recovery (Robleto et al., 2004; Delamater, 2004; Bouton, 2004; Rescorla, 2004;
180 Thanellou & Green, 2011). The CR extinction profiles (Fig. 4C) could be fitted to single
181 exponential curves, as characterized by the following equation:

182 $$\%CR = P_{ext} * \exp\left(-\frac{N_{CS}}{\tau_{ext}}\right)$$

183 , where P_{ext}, τ_{ext} and N_{CS} represent the initial value of %CR, the factor for resistance of
184 CR to be extinct, and the number of CS-alone trials during each day, respectively. The CRs
185 established by rich paired stimuli seem to exhibit ~4 times greater resistance to extinction in mice,
186 which is distinct from humans showing higher resistance in partial reinforcement-acquired CRs
187 (Grant & Schipper, 1952; Humphreys, 1939; Grant & Hake, 1951; Moore & Gormezano, 1963)
188 and also rabbits with almost similar resistance irrespective of sensory enrichment during
189 acquisition (Thomas & Wagner, 1964; Gormezano & Coleman, 1975). In clear contrast to
190 the %CR attenuation (i.e., reduction in percentage of occurrence), eyelid closure amplitude, if
191 occurred, was kept high during the extinction sessions in all groups, although the 11 trials group
192 showed slight decline (Fig. 4D, E). Furthermore, interestingly, eye blinking like spontaneous

193 responses tended to be frequently observed during extinction (Fig. S3C, 4F, G). As for the timing
194 control, response onset showed delay during extinction although peak latency exhibited large
195 variabilities among individuals (Fig. 4H), as previously reported (Kehoe et al., 2014; Medina et
196 al., 2002). Taken together, eyeblink extinction learning is expressed as purely decreased
197 probability, without changing the behavior dynamics, of blinking in response to the repetitive
198 tone-alone experience, implying the preserved memory for well-timed blinking in the neuronal
199 circuit, in line with the idea that the CR extinction is mediated by formation of new memory to
200 counteract the CR occurrence (Kim et al., 2020).
201
202 **Modeling CR acquisition and extinction through integrating total history of sensory inputs**
203 To shed light on the underlying mechanisms of distinct dynamics of CR acquisition and extinction
204 with altered pairings of sensory stimuli, we attempted to develop a model that explains our
205 observations (see Figs. 1 and 4). Several lines of evidences in our experiments, such as the
206 apparent differences in rate of acquisition, saturated level, but preserved eyeblink dynamics and
207 the daily spontaneous recovery during extinction (see Fig. 4), indicated interaction of
208 independently established two memory components for CR, one encoding execution and the other
209 suppression, as previously suggested (Robleto et al., 2004; Delamater, 2004; Bouton, 2004;
210 Rescorla, 2004; Felsenberg et al., 2018). Thus, we built a model assuming parallel formation of
211 counteracting memories for CRs, as follows (here, in modeling section, we denote %CR as
212 CR_{ratio}):

213 $$CR_{ratio} = v1_{2nd} + v1_{1st} * (1 - g * v2)$$

214 $$v1 = v1_{1st} + v1_{2nd}$$

215 , where $v1$ is the memory for CR execution consisting of two components, $v1_{1st}$ and $v1_{2nd}$
216 with distinct susceptivity to the CR suppressing memory, $v2$. g represents a gate for $v2$, increasing

as a function of total amount of CS inputs (i.e. total trial number) (Fig. 5A; for details see Materials and Methods). The larger $v1$ results in higher CR_{ratio}, while the larger $v2$ leads to smaller CR_{ratio}. $v1_{1st}$, $v1_{2nd}$ and $v2$ were assumed to build up trial by trial based on the Rescorla and Wagner model (Rescorla & Wagner, 1972) with some modification, defined as follows:

$$\Delta v1_{1st} = \alpha 1_{1st} * \beta * (\lambda 1 - v1) - \alpha 1_{2nd} * v1_{1st} \qquad \text{[upon CS-US]}$$

$$\Delta v1_{2nd} = \alpha 1_{2nd} * v1_{1st} \qquad \text{[upon CS-US]}$$

$$\Delta v2 = \alpha 2 * (\lambda 2 - v2) \qquad \text{[upon CS-alone]}$$

, where $\alpha 1_{1st}$, $\alpha 1_{2nd}$ and $\alpha 2$ represent rate constants for formation of memories $v1_{1st}$, $v1_{2nd}$ and $v2$, respectively. $v1_{1st}$ was assumed to be formed upon the CS-US pairings at a rate $\alpha 1_{1st}$ multiplied by an efficiency factor β, and to be gradually turned into the extinction-resistant $v1_{2nd}$ at a rate $\alpha 1_{2nd}$. Stronger resistance of CR to extinction in the $90\%_{\text{CS-US}}$ was made possible by this scheme (see Fig. 4C). Daily upper limit of learning, inferred from Fig. 1G, was implemented in the model by gradual decline of the $\alpha 1_{1st}$ efficiency factor β as total paired trials increase within a session (Fig. S5A).

Both the acquisition and extinction processes of CR_{ratio} were simulated in the model, and distinct dynamics for three experimentally-tested patterns were nicely reproduced (Fig. 5B-F). The $90\%_{\text{CS-US}}$ group hit daily plateau of CR acquisition, whereas the 11 trials group showed more efficient learning as observed in experiments. In the $10\%_{\text{CS-US}}$ group, even after reaching apparent saturation, CR_{ratio} exhibited daily quick increase and following "within-session decline" because of gradual gating of slowly summating $v2$ to counteract $v1_{1st}$ via activation of g by repeated trials (Fig. 5B, E, F).

We also conceived another model in which the suppressing memory, $v2$ was short-lived and refreshed by the next session, rather than long-lasting (compare Fig. S6B with Fig. 5E). As shown in Fig. S6A, this model also succeeded in reproducing experimental observations. In this

241 version, notably, daily spontaneous recovery during extinction sessions can be explained just by
242 the complete refreshment of *v2* irrespective of the inclusion of a gating mechanism of *v2* (Fig.
243 S6B, C). However, the "within-session decline" during acquisition in the $10\%_{CS\text{-}US}$ was still
244 strongly dependent on the gating mechanism: eliminating the gate made the "within-session
245 decline" more rapid and potent than actual experimental data (Fig. S6C). Thus, in any cases, the
246 memory *v2* to suppress CRs are to be adequately controlled by the online experience of sensory
247 inputs, as has been suggested in a previous study showing that the decline of %CR speeded down
248 with occasional paired sensory inputs during the extinction session (Gibbs et al., 1978).
249

250 **Model-driven discovery of prior-formed suppression memory**

251 To evaluate the qualitative difference of learning dynamics generated by two *v2,* characterized
252 with distinct temporal lifetime, long- or short-lasting one, we attempted to obtain a prediction
253 from the two models. Repetitive CS-alone trials presented for days in prior suppressed the later
254 CR_{ratio} increase in the model with long-lasting *v2*, but not in the model assuming short-lasting *v2*
255 (Fig. 6A). Thus, the modeling analysis yielded a prediction: if long-lasting, the suppressing
256 memory *v2* can be formed in prior to the start of CR acquisition. This prediction was tested by
257 behavioral experiments presenting 100 CS-alone trials for 4 days prior to the start of 90% CS-US
258 pairing paradigm (the Pre group). Strikingly consistent with the model prediction, as shown in
259 Fig. 6A and B, the Pre CS-alone trials potently inhibited the initial growth of CRs, which has also
260 been known as latent inhibition (Lubow & Moore, 1959; Schmajuk et al., 1994; Nicholson &
261 Freeman, 2002), without affecting the dynamics of acquired eyelid closure (Fig. 6C). Furthermore,
262 despite the later training paradigm by itself was the 90% pairing of CS and US, surprisingly, the
263 increase of %CR in the Pre-group showed quite similar pattern to that in the $10\%_{CS\text{-}US}$ groups
264 rather than the $90\%_{CS\text{-}US}$ (Fig. 6B), characterized by "within-session decline" (Fig. 6D).

Accordingly, the zig-zag pattern in CR_{ratio} dynamics was more evident in the model with long-lasting *v2* (Fig. 6A). Thus, the prediction of model assuming long-lasting v2 was validated by the animal behavior experiments, and amazingly it was revealed that even before the acquisition of CRs, the prior experience of CS-alone inputs forms negative counteracting memory for not only the later acquisition but also the execution probability of CRs after acquisition, as if the CR memory was established through the limited pairings. Collectively, we conclude that the association of CS and US forms a memory to execute CRs, while CS-alone experience forms a counteracting long-term memory to suppress CRs in parallel and independently from the situation of the target positive memory.

Discussion

Changing the training paradigm of cerebellum-dependent eyeblink conditioning, here we demonstrated that the learning efficiency is paradoxically facilitated by restricting the number of daily trainings. Distinct occurrence profiles of the learned behavior without changes in blinking dynamics during the acquisition and extinction highlighted the sensory experience-dependent parallel formation of long-term memories for the CR execution and its suppression. The different counteraction of the two memories explained patterns of acquired behavior occurrence with distinct sensory experience in acquisition, extinction, and even latent inhibition. Thus, our present study provides a previously unprecedented simple framework for learning assuming only two memories, by which distinct sensory experiences in combination and timeline can be integrated in animals brain.

CR acquisition with partial reinforcement

289 Eyeblink conditioning is conserved widely in mammals, showing specie-dependent different
290 relations between the training patterns and the learning dynamics. Humans show %CR closely
291 related to the ratio of pairings (Grant & Schipper, 1952; Grant & Hake, 1951; Moore &
292 Gormezano, 1963; Ross, 1959), while rabbits supra-linearly exhibit CRs upon training with
293 smaller possibility of sensory pairings (Thomas & Wagner, 1964; Leonard & Theios, 1967;
294 Gormezano & Coleman, 1975; Buchanan et al., 1997). As demonstrated here, even much smaller
295 10% pairing is sufficient for the CR acquisition in mice (see Fig. 1F), showing rather inversed
296 relationship between the enrichment of associative experience and the learning efficiency (see
297 Fig. 1G), which contrasts to the previous findings in rabbits typically showing equal or less
298 efficiency with partial reinforcement (Thomas & Wagner, 1964; Leonard & Theios, 1967;
299 Gormezano & Coleman, 1975). Apparent slower growth of %CR in mice than in rabbits during
300 days of trainings (Thomas & Wagner, 1964; Heiney et al., 2014; Leonard & Theios, 1967;
301 Gormezano & Coleman, 1975; Fiocchi et al., 2022), implies more potent upper limit of learning
302 during a certain period in mice, spoiling surplus reinforcement experience. This could be
303 responsible for the apparent higher learning efficiency upon limited reinforcement. Indeed,
304 learning efficiency can be estimated higher also in rabbits with smaller density of training, when
305 compared with a training paradigm accompanied with daily saturation or decline of %CR (Tait et
306 al., 1983; Kehoe & White, 2002).
307

308 **Candidates for neural circuits generating distinct profiles in CR execution**

309 We demonstrated a critical role of cerebellar circuit in expression of learned eyeblink irrespective
310 of the enrichment of reinforcement (Fig. 3; Christian & Thompson, 2003; Yeo et al., 1985;
311 McCormick et al., 1982; Krupa et al., 1993). Long-term depression (LTD) at parallel fiber (PF)
312 synapses on a Purkinje cell (PC) has been focused as a substrate of memory formation for CRs

313 (Koekkoek et al., 2003). In addition, plasticity at mossy fiber (MF) synapses on neurons in DCN
314 also plays a role, contributing to higher resistance to extinction presumably requiring more
315 experience for its establishment compared to PF-PC LTD (Garcia & Mauk, 1998; Medina et al.,
316 2001; Ohyama et al., 2006; Antonietti et al., 2016; Antonietti et al., 2017; Broersen et al., 2023).
317 Given these findings, the PF-PC LTD and plasticity at MF-DCN synapses might correspond to
318 the extinction-sensitive ($v1_{1st}$) and -resistant ($v1_{2nd}$) memories for CRs in our hypothetical model
319 (see Fig. 5A).

320 While classical Rescorla-Wagner models account for the net associative strength, our
321 findings necessitate a model with dual, independent components to explain the dissociable
322 kinetics of CR acquisition and its within-session suppression, as previously suggested as
323 independent memory formation for extinction of learned behavior (Robleto et al, 2004; Delamater,
324 2004; Bouton, 2004; Rescorla, 2004; Felsenberg et al., 2018). Accordingly, our experiments and
325 modeling together highlighted an importance of the memory counteracting CR execution, not
326 only for the extinction, but also for the fine-tuned probability to execute learned eyelid closure.
327 In addition, surprisingly, our data suggest that the inhibitory memory trace ($v2$) can be somehow
328 long-lasting and formed even prior to the formation of positive memory to execute eyeblink.
329 Crucially, our model's prediction that the inhibitory memory trace can be surreptitiously
330 established even in the absence of behavioral CR was empirically validated. Thus, $v2$ seems to
331 practically underlie the lowered efficiency in acquisition after the prior CS presentations, known
332 as latent inhibition (Lubow & Moore, 1959; Schmajul et al., 1994; Nicholson & Freeman, 2002).
333 Recently, it was demonstrated in *Drosophila* that odor pre-exposure forms an independent
334 aversive memory that competes with subsequent learning, providing a mechanistic basis for latent
335 inhibition and also extinction learning (Jacob et al., 2021). Our results extend this concept to the
336 mammalian cerebellum, demonstrating that such "pre-emptive" inhibitory memories are not only

formed prior to acquisition but also dynamically interact with excitatory traces to fine-tune motor outputs on a trial-by-trial basis.

One candidate mechanism of the inhibitory memory trace in the cerebellum is long-term potentiation (LTP) between PF and PC in cerebellum (Kim et al., 2020; De Zeeuw, 2021; Kostadinov & Häusser, 2022). Cerebellar extinction was shown to involve a reversal of synaptic plasticity, such as the transition from LTD to LTP at PF-PC synapses, driven by the deprivation of climbing fiber signals (Medina et al., 2002). Our present study presented another suppressing process for the memory under conditions of sparse reinforcement: independent inhibitory memory (*v2*) tunes the behavior while keeping robust excitatory memories (*v1*). It is conceivable that LTD and LTP at PF-PC synapses are formed at distinct micro-zones (De Zeeuw, 2021; Kostadinov & Häusser, 2022), and outputs from these PCs counteract at identical DCN neurons. This bidirectional control of learning gain resonates with the cellular mechanisms proposed for vestibulo-ocular reflex (VOR) adaptation, where the balance between LTD and LTP at PF-PC synapses mediates the up- and down-regulation of motor gain (Raymond and Lisberger, 1998; Boyden and Raymond, 2003). While VOR adaptation is often explained by the shifting balance of these opposing plasticities within a single pathway, our findings in eyeblink conditioning extend this concept by demonstrating that 'gain' can also be regulated through the parallel accumulation of an independent inhibitory memory. In our model, the '10% reinforcement' advantage is not merely a result of less synaptic saturation, but an manifestation of an optimized gain control where the inhibitory memory (*v2*) prevents excessive responding without erasing the excitatory trace. This suggests a universal principle in cerebellar computation: whether through bidirectional plasticity at a single synapse or through the parallel recruitment of opposing memory pathways, the cerebellum actively calibrates its output gain to match the statistical structure of environmental feedback. Alternatively, the suppression of CR-executing processing might be

enabled in the cerebellar circuit by dynamic plasticity at GABAergic synapses, for example between molecular layer interneurons and PCs (Kawaguchi & Hirano, 2000) and/or those between PCs and neurons in DCN (Aizenman et al., 1998). In addition, outside of cerebellum, CR extinction-related hippocampus (Schmaltz & Theios, 1972; Akase et al., 1989), or dopaminergic signals from ventral tegmental area (VTA) to nucleus accumbens (Kutlu et al., 2022) and posterior part of striatum (Menegas et al., 2017) related to latent inhibition might affect plasticity at various synapses in the cerebellar cortex and nuclei.

Our present data demonstrated that negative effects on CR execution in the latent inhibition, extinction, and "within-session decline", could be integrated into the sole inhibitory memory trace *v2* in the simple framework (see Fig. 5A), which corresponds to mechanistic clarification of the nature of a century debate on the latent inhibition, primarily explained as the lowered attention. Gating of such an inhibitory memory across past, online, and ongoing sensory events highlights that the cerebellum constantly integrates sensory history to calibrate future motor outputs. Taken all these findings together, by shedding light on the counteractions of opposite memories integrating distinct sensory inputs, the present study opens a door to clarify the key neuronal mechanism to fine-tune the learned behavior reflecting the whole history of experience, not only for eyeblink conditioning but also for other associative learning paradigms like fear conditioning and reward-related reinforced learning.

380 **Materials & Methods**

381 **Animal usages**

382 Adult male FVB/NJcl mice, ≥ 8 weeks old, were used in all experiments (n = 86). Mice were
383 housed singly with *ad libtum* access to food and water in a room with 12 hours of light/dark cycle.
384 All animal procedures were performed by the same experimenter in accordance with guidelines
385 on animal experimentation in Kyoto University and approved by the local committee in Graduate
386 School of Science, Kyoto University.

387

388 **Surgery**

389 Custom-made aluminum head-plates were mounted on mice before experiments. Mice were
390 anesthetized with intraperitoneal injection (0.2-0.3 ml/mouse) of mixture of 0.9% ketamine
391 (Daiichisankyo) and 0.2% xylazine (Bayer). The scalp was cut off to expose the skull and mice
392 were stereotaxically fixed on an operating table (Narishige). The underlying membranous tissue
393 was removed with cotton swabs and small holes were made around bregma using a drill. Screws
394 were loosely tightened to the holes. The head plate was placed on the skull surface and fixed to
395 the screws and the skull with dental cement (UNIFAST Trad, GC). Mice had at least 30 hours of
396 recovery period before experiments started.

397 To pharmacologically inactivate DCN, a guide cannula (RWD Life Science) was
398 implanted for some mice (n = 12) together with a head plate (see Fig. 3A). A small hole (~6.0 mm
399 posterior, ~2.0 mm lateral from bregma; Paxinos & Franklin, 2008) was drilled and the cannula
400 tip was approached to the brain surface using a stereotaxic micromanipulator. The cannula was
401 inserted 1.8-2.3 mm vertically and fixed with dental cement. An internal dummy cannula was
402 inserted to the guide cannula to prevent clogging.

403

404 **Eyeblink conditioning, acquisition and extinction**

405 The basic apparatus was composed of a self-made treadmill on which mice were head-fixed
406 during experiments, a camera (CS135MU, Thorlabs) for eyelid closure recording, a speaker for
407 tone stimuli, a solenoid for air stimuli, and a PC (XPS8940, Dell) for recording and stimuli control
408 (Fig. S7A; Heiney et al., 2014). The treadmill was composed of cylindrical rotating rods and
409 rubber sheet. The implanted head-plate was fixed to a manipulator (SM-19, Narishige) ~2 cm
410 above the treadmill with a screw (Fig. 1C). The camera was mounted on a metal rod to monitor a
411 left eye. Mice were illuminated by white LED light and eyelid movements were recorded with
412 100 frames/sec. The speaker was placed back left side of mice. A gas cylinder was connected to
413 the solenoid and air was delivered to a left cornea when the solenoid opened. The camera, speaker
414 and solenoid were controlled in timing with Python through an AD/DA converter (DIO-8/8B-
415 UBT, Y2 Corporation).

416 Mice were randomly divided into three groups with distinct trainings ($90\%_{CS\text{-}US}$, n = 22;
417 $10\%_{CS\text{-}US}$, n = 20; 11 trials, n = 22), as follows (see Fig. 1A): $90\%_{CS\text{-}US}$ group, 10 blocks of 10
418 trials per day, with each block composed of 9 paired & 1 CS-alone trials; $10\%_{CS\text{-}US}$ group, 10
419 blocks of 1 paired & 9 CS-alone trials; 11 trials group, 10 paired & 1 CS-alone trials per day. Each
420 mouse had at least 6 days of training. Mice had habituation period without recording and stimuli
421 delivery for $\geq$ 15minutes on the treadmill before training each day. The CS (tone, 3.5 kHz, 75
422 dB, 290 ms) was co-terminated with the US (air puff, 15-30 psi, 40 ms) in CS-US paired trials;
423 on the other hand, the tone CS was given without the US presentation in CS-alone trials (Fig. 1A).
424 The US was delivered via a glass tube (i.d. = 0.5 mm) or a 21 gauge needle placed ~2 mm away
425 from a mouse cornea (Fig. 1C) and given in an almost identical manner through experiments
426 except for gradual increase in pressure as days of training proceeded (Fig. S7B). The order of
427 paired and CS-only trials was randomly determined in each block. The inter-trial interval was set

428 to 10-24 sec randomly for each trial.

429 Some mice (90%$_{CS\text{-}US}$, n = 8; 10%$_{CS\text{-}US}$, n = 9; 11 trials, n = 7) had 4 consecutive days of
430 extinction paradigm, 100 CS-alone trials/day, following the 10 consecutive days of acquisition.
431 Other mice (n = 8) had exposure to daily 100 CS-alone trials for 4 consecutive days prior to the
432 90%$_{CS\text{-}US}$ trainings (Pre group). When training was accidentally interrupted in the first block
433 because of system' s error, although very rare, daily traning was started over again.

434

435 **Data analysis**

436 Recorded videos for eyelid movements were converted into numerical trace by calculating the
437 area of an eyeball in individual frames (Fig. 1D; Heiney et al., 2014). Full eyelid open/close
438 corresponded to 0/100% respectively. Reflection of light and infiltration of whisker were
439 approximately calibrated. Trials were omitted from analysis when significant activities other than
440 eyelid closures were observed, or recording or saving of eyelid movements was not performed
441 properly. Eyelid closure amplitude was obtained by subtraction of pre-CS baseline from the
442 maximal eyelid closure during 80-250 ms after the CS onset (for CS-US paired trials) or 80-470
443 ms (for CS-alone trials). When the amplitude was $\geq$ 15%, this trial was regarded as one with a
444 response and further analysis was conducted. Onset of eyelid closure was visually identified. The
445 α-startle, a startle reflex to tone, was carefully removed from the analysis by visual identification.
446 The responses with averaged eyelid closure amplitude during 220-250 ms $\geq$ 15% and larger than
447 that during 120-150 ms, were regarded as CRs.

448

449 **Pharmacological inactivation of DCN neurons**

450 DCN neurons in CR-learned mice (90%$_{CS\text{-}US}$, n = 6; 10%$_{CS\text{-}US}$, n = 6) were inactivated by
451 muscimol (1 or 5 mM, Nakalai Tesque) administration through an implanted guide cannula (see

452 Surgery). Muscimol was diluted in aCSF (NaCl, 125 mM, $NaHCO_3$, 25 mM, NaH_2PO_4, 1.25 mM,
453 KCl, 2.5 mM, D-glucose, 10 mM, $CaCl_2 \cdot 2H_2O$, 2 mM, $MgCl_2 \cdot 6H_2O$, 2 mM, adjusted to pH ~7.4
454 and ~300 mOsm). An internal cannula connected to a microsyringe (701N 10 μl, Hamilton)
455 through silicon tube was inserted into the implanted guide cannula and muscimol (0.5-5 μl) was
456 infused (~1 μl/min). The internal cannula was removed carefully and the examination of eyelid
457 movements resumed within 15 mins. Mice were imposed ≥ 30 trials before/after the infusion.
458 In some mice ($90\%_{CS\text{-}US}$, n = 3; $10\%_{CS\text{-}US}$, n = 3), aCSF was infused without muscimol on another
459 day for negative control. The session was omitted from analysis when UR or ordinal behavior
460 significantly changed after the infusion.

461 Muscimol diffused area and the cannula position were confirmed in individual mice.
462 Acriflavine, a fluorescent dye, (0.5-5 μl, 0.01%, Wako), was infused in the same way as the
463 muscimol infusion ($90\%_{CS\text{-}US}$, n = 5; $10\%_{CS\text{-}US}$, n = 6) after pharmacological inactivation
464 experiments. Mice were euthanized by cervical dislocation and the head plates were detached
465 from the skulls. Whole brains were carefully removed and fixed in 4% paraformaldehyde/PBS
466 (paraformaldehyde: Nakalai Tesque; PBS: Takara Bio) overnight and soaked for >12 hours in
467 ~20% sucrose for cryoprotection. Horizontal sections were prepared at ~50 μm thickness using a
468 cryostat (SM2000R, Leica). These sections were immediately mounted (VECTARSHIELD
469 Mounting Medium, Funakoshi) and imaged with a confocal fluorescent microscope (FV1000,
470 Olympus). The area of muscimol diffusion was estimated from the acriflavine fluorescence. The
471 position of small holes in the sections was regarded as the positions of cannula.

472

473 **Modeling**

474 Learning model for CR acquisition and extinction was constructed, and the dynamics of
475 probability of CR occurrence was simulated under the Python programming language (Figs. 5, 6,

Figs. S5, S6). Memories for CR execution ($v1$) and suppression ($v2$) were assumed to be formed independently. As for $v1$, $v1_{1st}$ and $v1_{2nd}$ with distinct sensitivity to CR extinction or suppression were assumed based on the fact that the CRs showed resistance to extinction depending on the enrichment of paired sensory experiences (see Fig. 4C), together with the previous studies suggesting two candidate synapses encoding the CR-triggering memory with distinct resistance for extinction: synapses on cerebellar PCs and those in DCN (Garcia & Mauk, 1998; Medina et al., 2001; Ohyama et al., 2006; Antonietti et al., 2016; Antonietti et al., 2017; Broersen et al., 2023). On the other hand, trials-dependent gradual suppression by the memory $v2$, was implemented by the gate control 'g', which made the spontaneous recovery possible in the model.

Taken together, the CR_{ratio} was expressed as a function of three memories, as follows:

$$CR_{ratio} = v1_{2nd} + v1_{1st} * (1 - g * v2)$$

$$v1 = v1_{1st} + v1_{2nd}$$

Three memories, $v1_{1st}$, $v1_{2nd}$ and $v2$, changed trial by trial based on Rescorla-Wagner model (Rescorla & Wagner, 1972), as follows:

$$\Delta v1_{1st} = \alpha 1_{1st} * \beta * (\lambda 1 - v1) - \alpha 1_{2nd} * v1_{1st} \qquad \text{[upon CS-US]}$$

$$\Delta v1_{2nd} = \alpha 1_{2nd} * v1_{1st} \qquad \text{[upon CS-US]}$$

$$\Delta v2 = \alpha 2 * (\lambda 2 - v2) \qquad \text{[upon CS-alone]}$$

, where $\lambda 1$ and $\lambda 2$ are saturation levels for $v1$ and $v2$, and set to 1 here. $\alpha 1_{1st}$, $\alpha 1_{2nd}$, and $\alpha 2$ are rate constants for formation of $v1_{1st}$, $v1_{2nd}$ and $v2$, respectively. β was assumed here to make the CS-US pair-dependent formation of $v1_{1st}$ sensitive to the total number of daily paired trials within a session (N_{paired}) (Fig. S5A):

$$\beta = \frac{1}{1 + (\frac{N_{paired}}{\tau_\beta})^{n_\beta}}$$

, where τ_β and n_β define the steepness of experience-dependent slowing of $v1_{1st}$

formation.

Gating of suppressing memory *v2, g*, was also implemented as follows:

$$g = 1 - \frac{g_0}{1 + (\frac{N_{trial}}{\tau_{gate}})^{n_{gate}}}$$

, where N_{trial} is the total trial number in a session. g_0 is a factor to decide the initial gate active at the beginning of each session. τ_{gate} and n_{gate} define the steepness of the trials-dependent gate opening, and the former was defined to change depending on experience as follows (Fig. S5B):

$$\tau_{gate} = A_{gate} + B_{gate} * \frac{1}{1 + \left(\frac{p_\tau}{p(pair)_{exp}}\right)^{n_\tau}}$$

, where A_{gate} and B_{gate} are the initial value and the experience-dependent maximal increment of τ_{gate}, respectively. p_τ and n_τ are constants to define the steepness of τ_{gate} change. Expected paring ratio, $p(pair)_{exp}$, was assumed to be updated trial by trial as follows (Fig. S5C):

$$\Delta p(pair)_{exp} = \gamma * \left(1 - p(pair)_{exp}\right) \qquad \text{[upon CS-US]}$$

$$\Delta p(pair)_{exp} = \gamma * \left(0 - p(pair)_{exp}\right) \qquad \text{[upon CS-alone]}$$

, where γ is the rate constant for change of $p(pair)_{exp}$.

Individual memories were assumed to fade over time (t) as defined by the following equations:

$$\Delta v1_{1st} = -(1 - \frac{1}{1 + \left(\frac{t}{\varepsilon_{v1_1st}}\right)^{n_{decay}}}) * v1_{1st} + (1 - \frac{1}{1 + \left(\frac{t}{\varepsilon_{v1_2nd}}\right)^{n_{decay}}}) * v1_{2nd}$$

$$\Delta v1_{2nd} = -(1 - \frac{1}{1 + \left(\frac{t}{\varepsilon_{v1_2nd}}\right)^{n_{decay}}}) * v1_{2nd}$$

$$\Delta v2 = -(1 - \frac{1}{1 + \left(\frac{t}{\varepsilon_{v2}}\right)^{n_{decay}}}) * v2$$

, where ε_{v1_1st}, ε_{v1_2nd}, ε_{v2}, and n_{decay} are time constants of memory decay and their steepness. Daily decay of each was calculated before each session started in simulation using 1440 min, corresponding to 24 hours, for time t. Other variables, β, g, and $p(pair)_{exp}$ are refreshed to initial values at the beginning of each day (see Table S1).

Simulation was performed trial by trial, giving CS-US paired or CS-alone trials as in the experiments. The 2 models assuming long- or short- lasting *v2* suppressing memory, and a model without gate control were performed by changing corresponding parameters (see Table S1).

Statistics

Data was presented as mean ± SEM unless otherwise stated. Paired t-test and Tukey-Kramer test were performed with Microsoft Excel or Rstudio (Posit) for statistical analysis. *, $p < 0.05$; **, $p < 0.01$; ***, $p < 0.001$ were regarded as significant. Approximate curves were obtained with Igor Pro8 (WaveMetrics) using Chi-square method.

References

Aizenman, C.D., Manis, P.B., and Linden, D.J. (1998). Polarity of Long-Term Synaptic Gain Change Is Related to Postsynaptic Spike Firing at a Cerebellar Inhibitory Synapse. Neuron *21*, 827–835. https://doi.org/10.1016/S0896-6273(00)80598-X.

Akase, E., Alkon, D.L., and Disterhoft, J.F. (1989). Hippocampal lesions impair memory of short-delay conditioned eye blink in rabbits. Behavioral Neuroscience *103*, 935–943. https://doi.org/10.1037/0735-7044.103.5.935.

Antonietti, A., Casellato, C., D'Angelo, E., and Pedrocchi, A. (2017). Model-Driven Analysis of Eyeblink Classical Conditioning Reveals the Underlying Structure of Cerebellar Plasticity and Neuronal Activity. IEEE Trans. Neural Netw. Learning Syst. *28*, 2748–2762. https://doi.org/10.1109/TNNLS.2016.2598190.

Antonietti, A., Casellato, C., Garrido, J.A., Luque, N.R., Naveros, F., Ros, E., DAngelo, E., and Pedrocchi, A. (2016). Spiking Neural Network With Distributed Plasticity Reproduces Cerebellar Learning in Eye Blink Conditioning Paradigms. IEEE Trans. Biomed. Eng. *63*, 210–219. https://doi.org/10.1109/TBME.2015.2485301.

Balsam, P.D., Drew, M.R., and Yang, C. (2002). Timing at the Start of Associative Learning. Learning and Motivation *33*, 141–155. https://doi.org/10.1006/lmot.2001.1104.

Bologna, M., Paparella, G., Valls-Solé, J., Hallett, M., and Berardelli, A. (2024). Neural control of blinking. Clinical Neurophysiology *161*, 59–68. https://doi.org/10.1016/j.clinph.2024.02.023.

Bouton, M.E. (2004). Context and Behavioral Processes in Extinction. Learn. Mem. *11*, 485-494.

Boyden ES, and Raymond JL. (2003). Active reversal of motor memories reveals rules governing memory encoding. Neuron, 39, 1031-42. doi: 10.1016/s0896-6273(03)00562-2.

Broersen, R. (2023). Synaptic mechanisms for associative learning in the cerebellar nuclei. Nature Communications. *14*, 7459.

Buchanan, S.L., Penney, J., Tebbutt, D., and Powell, D.A. (1997). Lesions of the mediodorsal nucleus of the thalamus and classical eyeblink conditioning under less-than-optimal stimulus conditions: Role of partial reinforcement and interstimulus interval. Behavioral Neuroscience *111*, 1075–1085. https://doi.org/10.1037/0735-7044.111.5.1075.

Cason, H. (1922). The conditioned eyelid reaction. Journal of Experimental Psychology *5*, 153–196. https://doi.org/10.1037/h0074822.

576 Christian, K.M., and Thompson, R.F. (2003). Neural Substrates of Eyeblink Conditioning:
577 Acquisition and Retention. Learn. Mem. *10*, 427–455. https://doi.org/10.1101/lm.59603.
578
579 De Zeeuw, and I, C. (2021). Bidirectional learning in upbound and downbound microzones
580 of the cerebellum. Nat Rev Neurosci *22*, 92–110. https://doi.org/10.1038/s41583-020-
581 00392-x.
582
583 Delamater, A. (2004). Experimental extinction in Pavlovian conditioning: Behavioural and
584 neuroscience perspectives. The Quarterly journal of experimental psychology. B,
585 Comparative and physiological psychology *57*, 97–132.
586 https://doi.org/10.1080/02724990344000097.
587
588 Felsenberg, J., Jacob, P.F., Walker, T., Barnstedt, O., Edmondson-Stait, A.J., Pleijzier, M.W.,
589 Otto, N., Schlegel, P., Sharifi, N., Perisse, E., et al. (2018). Integration of Parallel Opposing
590 Memories Underlies Memory Extinction. Cell *175*, 709-722.e15.
591 https://doi.org/10.1016/j.cell.2018.08.021.
592
593 Fiocchi, F.R., Dijkhuizen, S., Koekkoek, S.K.E., De Zeeuw, C.I., and Boele, H.J. (2022).
594 Stimulus Generalization in Mice during Pavlovian Eyeblink Conditioning. eNeuro *9*,
595 ENEURO.0400-21.2022. https://doi.org/10.1523/ENEURO.0400-21.2022.
596
597 Garcia, K.S., and Mauk, M.D. (1998). Pharmacological analysis of cerebellar contributions to
598 the timing and expression of conditioned eyelid responses. Neuropharmacology *37*, 471–480.
599 https://doi.org/10.1016/S0028-3908(98)00055-0.
600
601 Gibbs, C.M., Latham, S.B., and Gormezano, I. (1978). Classical conditioning of the rabbit
602 nictitating membrane response: Effects of reinforcement schedule on response maintenance
603 and resistance to extinction. Animal Learning & Behavior *6*, 209–215.
604 https://doi.org/10.3758/BF03209603.
605
606 Gormezano, I., and Coleman, S.R. (1975). Effects of partial reinforcement on conditioning,
607 conditional probabilities, asymptotic performance, and extinction of the rabbit's nictitating
608 membrane response. Pav. J. Biol. Sci. *10*, 13–22. https://doi.org/10.1007/BF03000620.
609
610 Grant, D.A., and Hake, H.W. (1951). Dark adaptation and the Humphreys random
611 reinforcement phenomenon in human eyelid conditioning. Journal of Experimental
612 Psychology *42*, 417–423. https://doi.org/10.1037/h0057031.
613
614 Grant, D.A., and Schipper, L.M. (1952). The acquisition and extinction of conditioned eyelid
615 responses as a function of the percentage of fixed-ratio random reinforcement. Journal of
616 Experimental Psychology *43*, 313–320. https://doi.org/10.1037/h0057186.
617
618 Heiney, S.A., Wohl, M.P., Chettih, S.N., Ruffolo, L.I., and Medina, J.F. (2014). Cerebellar-

Dependent Expression of Motor Learning during Eyeblink Conditioning in Head-Fixed Mice. J. Neurosci. *34*, 14845–14853. https://doi.org/10.1523/JNEUROSCI.2820-14.2014.

Humphreys, L.G. (1939). The effect of random alternation of reinforcement on the acquisition and extinction of conditioned eyelid reactions. Journal of Experimental Psychology *25*, 141–158. https://doi.org/10.1037/h0058138.

Jacob, P.F., Vargas-Gutierrez, P., Okray, Z., Vietti-Michelina, S., Felsenberg, J., and Waddell, S. (2021). Prior experience conditionally inhibits the expression of new learning in Drosophila. Current Biology *31*, 3490-3503.e3. https://doi.org/10.1016/j.cub.2021.05.056.

Kaminer, J., Powers, A.S., Horn, K.G., Hui, C., and Evinger, C. (2011). Characterizing the Spontaneous Blink Generator: An Animal Model. J. Neurosci. *31*, 11256–11267. https://doi.org/10.1523/JNEUROSCI.6218-10.2011.

Kaminer, J., Thakur, P., and Evinger, C. (2015). Effects of subthalamic deep brain stimulation on blink abnormalities of 6-OHDA lesioned rats. Journal of Neurophysiology *113*, 3038–3046. https://doi.org/10.1152/jn.01072.2014.

Kawaguchi, S., and Hirano, T. (2000). Suppression of Inhibitory Synaptic Potentiation by Presynaptic Activity through Postsynaptic GABAB Receptors in a Purkinje Neuron. Neuron *27*, 339–347. https://doi.org/10.1016/S0896-6273(00)00041-6.

Kehoe, E.J., Ludvig, E.A., Dudeney, J.E., Neufeld, J., and Sutton, R.S. (2008). Magnitude and timing of nictitating membrane movements during classical conditioning of the rabbit (Oryctolagus cuniculus). Behavioral Neuroscience *122*, 471–476. https://doi.org/10.1037/0735-7044.122.2.471.

Kehoe, E.J., Ludvig, E.A., and Sutton, R.S. (2014). Time course of the rabbit's conditioned nictitating membrane movements during acquisition, extinction, and reacquisition. Learn. Mem. *21*, 585–590. https://doi.org/10.1101/lm.034504.114.

Kehoe, E.J., and White, N.E. (2002). Extinction revisited: Similarities between extinction and reductions in US intensity in classical conditioning of the rabbit's nictitating membrane response. Animal Learning & Behavior *30*, 96–111. https://doi.org/10.3758/BF03192912.

Kim, O.A., Ohmae, S., and Medina, J.F. (2020). A cerebello-olivary signal for negative prediction error is sufficient to cause extinction of associative motor learning. Nat Neurosci *23*, 1550–1554. https://doi.org/10.1038/s41593-020-00732-1.

Koekkoek, S.K.E., Hulscher, H.C., Dortland, B.R., Hensbroek, R.A., Elgersma, Y., Ruigrok, T.J.H., and De Zeeuw, C.I. (2003). Cerebellar LTD and Learning-Dependent Timing of Conditioned Eyelid Responses. Science *301*, 1736–1739.

https://doi.org/10.1126/science.1088383.

Kostadinov, D., and Häusser, M. (2022). Reward signals in the cerebellum: Origins, targets, and functional implications. Neuron *110*, 1290–1303. https://doi.org/10.1016/j.neuron.2022.02.015.

Krupa, D.J., Thompson, J.K., and Thompson, R.F. (1993). Localization of a Memory Trace in the Mammalian Brain. Science *260*, 989–991. https://doi.org/10.1126/science.8493536.

Kutlu, M.G., Zachry, J.E., Melugin, P.R., Tat, J., Cajigas, S., Isiktas, A.U., Patel, D.D., Siciliano, C.A., Schoenbaum, G., Sharpe, M.J., et al. (2022). Dopamine signaling in the nucleus accumbens core mediates latent inhibition. Nat Neurosci *25*, 1071–1081. https://doi.org/10.1038/s41593-022-01126-1.

Leonard, D.W., and Theios, J. (1967). Classical eyelid conditioning in rabbits under prolonged single alternation conditions of reinforcement. Journal of Comparative and Physiological Psychology *64*, 273–276. https://doi.org/10.1037/h0088043.

Lubow, R.E., and Moore, A.U. (1959). Latent inhibition: The effect of nonreinforced pre-exposure to the conditional stimulus. Journal of Comparative and Physiological Psychology *52*, 415–419. https://doi.org/10.1037/h0046700.

McCormick, D.A., Clark, G.A., Lavond, D.G., and Thompson, R.F. (1982). Initial localization of the memory trace for a basic form of learning. Proc. Natl. Acad. Sci. U.S.A. *79*, 2731–2735. https://doi.org/10.1073/pnas.79.8.2731.

McCormick, D.A., and Thompson, R.F. (1984). Cerebellum: Essential Involvement in the Classically Conditioned Eyelid Response. Science *223*, 296–299. https://doi.org/10.1126/science.6701513.

Medina, J.F., Nores, W.L., and Mauk, M.D. (2002). Inhibition of climbing fibres is a signal for the extinction of conditioned eyelid responses. Nature *416, 330-333*.

Medina, J.F., Garcia, K.S., and Mauk, M.D. (2001). A Mechanism for Savings in the Cerebellum. J. Neurosci. *21*, 4081–4089. https://doi.org/10.1523/JNEUROSCI.21-11-04081.2001.

Menegas, W., Babayan, B.M., Uchida, N., and Watabe-Uchida, M. (2017). Opposite initialization to novel cues in dopamine signaling in ventral and posterior striatum in mice. eLife *6*, e21886. https://doi.org/10.7554/eLife.21886.

Moore, J.W., and Gormezano, I. (1963). Effects of omitted versus delayed UCS on classical eyelid conditioning under partial reinforcement. Journal of Experimental Psychology *65*, 248–

257. https://doi.org/10.1037/h0040671.

Nicholson, D., and Freeman, J. (2002). Medial Dorsal Thalamic Lesions Impair Blocking and Latent Inhibition of the Conditioned Eyeblink Response in Rats. Behavioral neuroscience *116*, 276–285. https://doi.org/10.1037/0735-7044.116.2.276.

Ohyama, T., and Mauk, M.D. (2001). Latent Acquisition of Timed Responses in Cerebellar Cortex. J. Neurosci. *21*, 682–690. https://doi.org/10.1523/JNEUROSCI.21-02-00682.2001.

Ohyama, T., Nores, W.L., Medina, J.F., Riusech, F.A., and Mauk, M.D. (2006). Learning-Induced Plasticity in Deep Cerebellar Nucleus. J. Neurosci. *26*, 12656–12663. https://doi.org/10.1523/JNEUROSCI.4023-06.2006.

Paxinos, G., and Franklin, K.B.J. (2008). The Mouse Brain in Stereotaxic Coordinates, Compact, Third Edition: The coronal plates and diagrams. (Academic Press).

Raymond JL, and Lisberger SG. (1998). Neural learning rules for the vestibulo-ocular reflex. J Neurosci. 18, 9112-29. doi: 10.1523/JNEUROSCI.18-21-09112.1998.

Rescorla, R., and Wagner, A. (1972). A theory of Pavlovian conditioning: Variations in the effectiveness of reinforcement and nonreinforcement. In Classical Conditioning II: Current Research and Theory. (Appleton Century Crofts).

Rescorla, R.A. (2004). Spontaneous Recovery. Learn. Mem. *11*, 501–509. https://doi.org/10.1101/lm.77504.

Robleto, K., Poulos, A.M., and Thompson, R.F. (2004). Brain Mechanisms of Extinction of the Classically Conditioned Eyeblink Response. Learn. Mem. *11*, 517–524. https://doi.org/10.1101/lm.80004.

Ross, L.E. (1959). The decremental effects of partial reinforcement during acquisition of the conditioned eyelid response. Journal of Experimental Psychology *57*, 74–82. https://doi.org/10.1037/h0046965.

Sakamoto, T., and Endo, S. (2008). GABAA receptors in deep cerebellar nuclei play important roles in mouse eyeblink conditioning. Brain Research *1230*, 125–137. https://doi.org/10.1016/j.brainres.2008.06.079.

Schmajuk, N.A., Lam, Y.-W., and Christiansen, B.A. (1994). Latent inhibition of the rat eyeblink response: Effect of hippocampal aspiration lesions. Physiology & Behavior *55*, 597–601. https://doi.org/10.1016/0031-9384(94)90122-8.

Schmaltz, L.W., and Theios, J. (1972). Acquisition and extinction of a classically conditioned

response in hippocampectomized rabbits (Oryctolagus cuniculus). Journal of Comparative and Physiological Psychology *79*, 328–333. https://doi.org/10.1037/h0032531.

Tait, R.W., Kehoe, E.J., and Gormezano, I. (1983). Effects of US duration on classical conditioning of the rabbit's nictitating membrane response. Journal of Experimental Psychology: Animal Behavior Processes *9*, 91–101. https://doi.org/10.1037/0097-7403.9.1.91.

Thanellou, A., and Green, J.T. (2011). Spontaneous Recovery But Not Reinstatement of the Extinguished Conditioned Eyeblink Response in the Rat. Behav Neurosci *125*, 613–625. https://doi.org/10.1037/a0023582.

Thomas, E., and Wagner, A.R. (1964). PARTIAL REINFORCEMENT OF THE CLASSICALLY CONDITIONED EYELID RESPONSE IN THE RABBIT. J Comp Physiol Psychol *58*, 157–158. https://doi.org/10.1037/h0048811.

Yeo, C.H., Hardiman, M.J., and Glickstein, M. (1985). Classical conditioning of the nictitating membrane response of the rabbit. Exp Brain Res *60*, 87–98. https://doi.org/10.1007/BF00237022.

Acknowledgments

We thank Drs T. Inoshita and H. Hirai for the critical reading of the manuscript and helpful comments.

Funding

Japan Society for Promotion of Science, KAKENHI grants 22H02721 (SK)

Japan Society for Promotion of Science, KAKENHI grants 22K19360 (SK)

Japan Society for Promotion of Science, KAKENHI grants 25H02611 (SK)

Japan Society for Promotion of Science, KAKENHI grants 25K02362 (SK)

Takeda Science Foundation (SK)

JST SPRING JPMJSP2110 (RI)

Author contributions

Conceptualization: RI, SK; Investigation: RI; Visualization: RI, SK; Supervision: SK; Writing - original draft: RI, SK; Writing – review & editing: RI, SK

Competing interests

The authors declare that the research was conducted in the absence of any commercial or financial relationships that could be construed as a potential conflict of interest.

Data and materials availability

All data are available in the main text or the supplementary materials. Program codes for CR behavior simulation are also available on the website of the corresponding author (www.nb.biophys.kyoto-u.ac.jp/model).

Supplementary materials

Figs. S1 to S7

Table S1

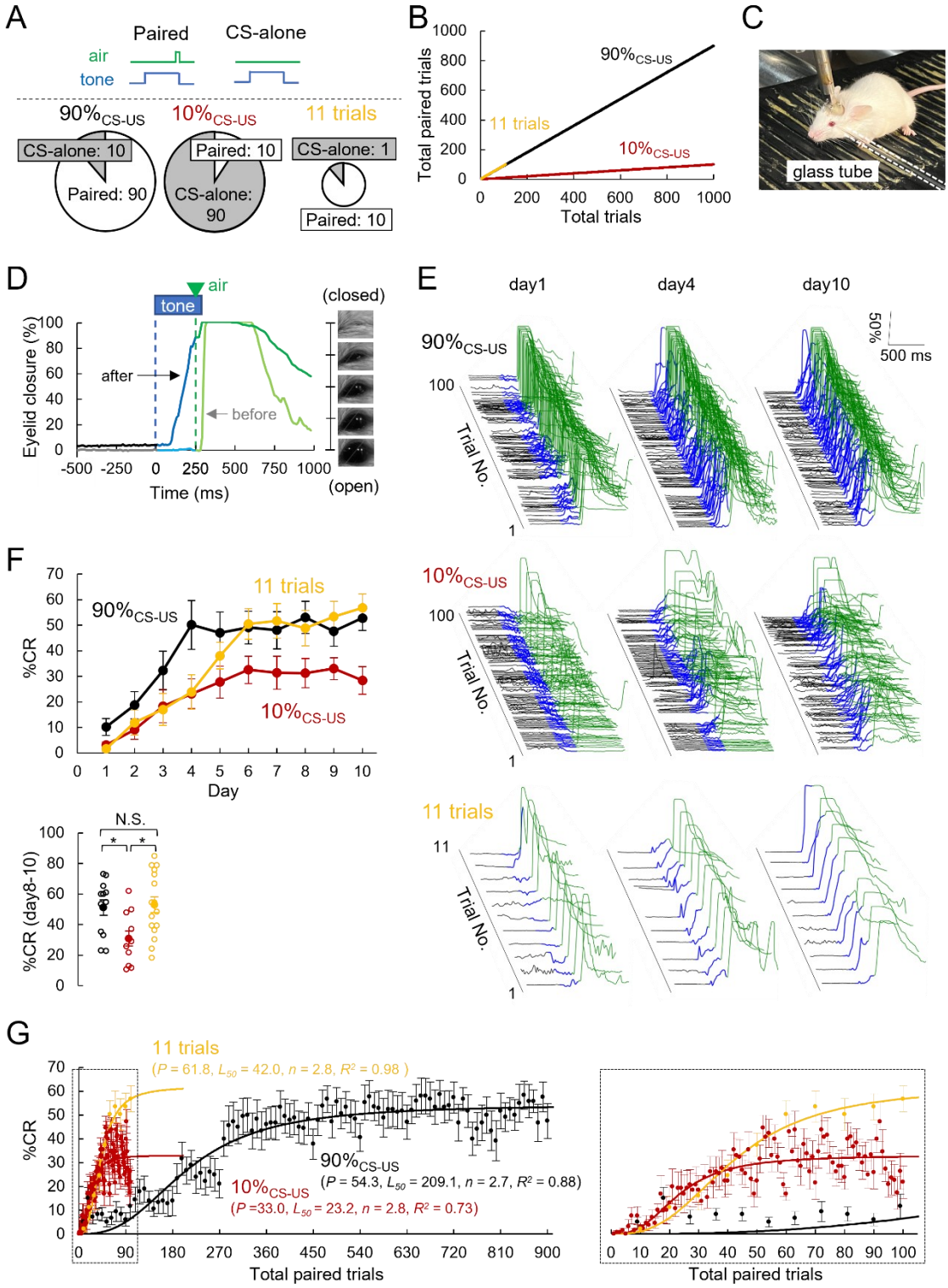

Fig 1. Eyeblink conditioning with distinct patterns of sensory pairings

(A) Schematics of CS (tone)-US (air puff) and CS-alone trials (top) and three training protocols, 90%$_{CS\text{-}US}$, 10%$_{CS\text{-}US}$, and 11 trials (bottom). **(B)** Total paired trials number plotted against total

trials during 10 days training (90%$_{CS\text{-}US}$, black; 10%$_{CS\text{-}US}$, red; 11 trials, orange). (**C**) An image of a head-fixed mouse on a treadmill during experiments. A glass tube put in front of the eyelid is outlined by white dashed line. (**D**) Representative images and time courses of eyelid closure before/after the CR acquisition trainings. (**E**) Representative eyelid traces (100 or 11 trials from a single mouse) for the 90%$_{CS\text{-}US}$ (top), 10%$_{CS\text{-}US}$ (middle) and 11 trials (bottom) on day1 (left), 4 (middle) and 10 (right). (**F**) Daily changes of %CR established by 10 days training (top) and averaged %CR during day8-10 (bottom; 90%$_{CS\text{-}US}$: 51.1 ± 5.0%, n = 12; 10%$_{CS\text{-}US}$: 30.9 ± 4.9%, n = 11; 11 trials: 53.0 ± 5.1%, n = 16, *, $p < 0.05$ by Tukey-Kramer test), from mice showing CR establishment (CR ≥ 10% in at least 3 days). Individual, open circle; average, filled circle. (**G**) %CR averaged from each 10 or 11 trials plotted against the number of total paired trials (90%$_{CS\text{-}US}$, n = 18; 10%$_{CS\text{-}US}$, n = 13; 11 trials, n = 17). Fitted curves are also shown.

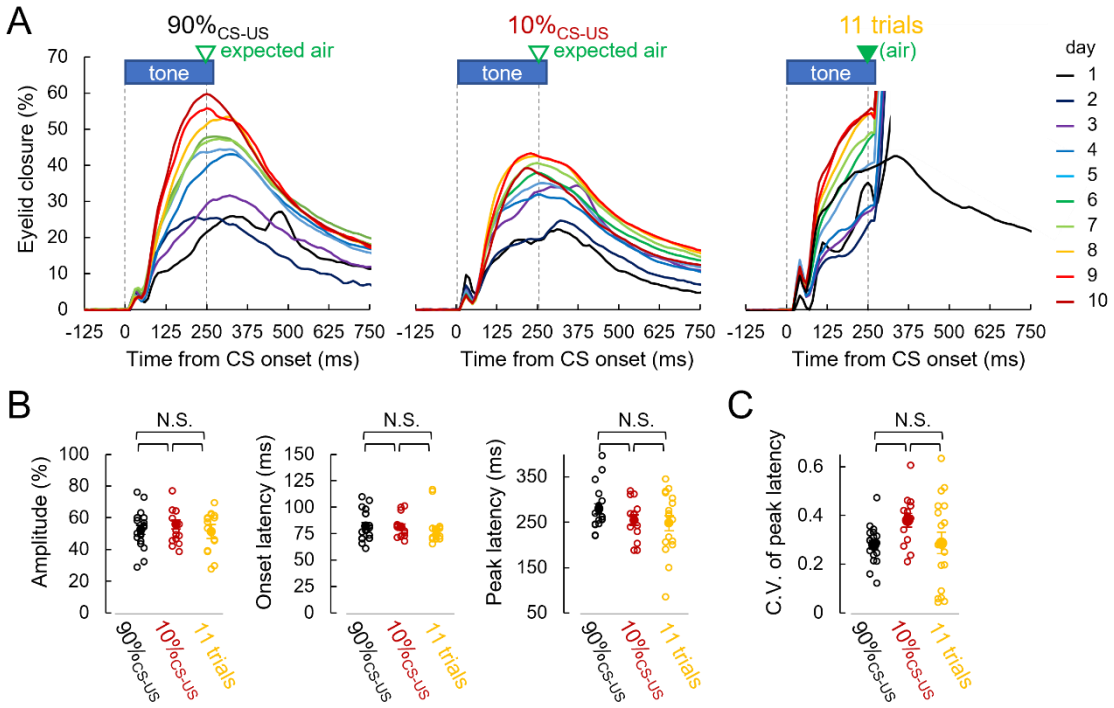

Fig 2. Learned eyelid responses

(A) Time courses of averaged eyelid closure for each day (90%$_{CS\text{-}US}$: n = 18 obtained from CS-alone trials; 10%$_{CS\text{-}US}$: n = 13 from CS-alone trials; 11 trials: n = 17 from paired & CS-alone trials). For 11 trials, a black trace obtained from averaging eyelid closures in CS-alone trials during 10 days is also shown. For averaging, only eyelid traces showing responses were used. Baseline level before CS was aligned to 0% for each. (**B**, **C**) Averaged amplitude (left), onset latency (middle) and peak latency (right) of eyeblink responses (B), and coefficient of variance for peak latency (C) obtained from all trials with responses. Individual, open circle; average, filled circle. Tukey-Kramer test.

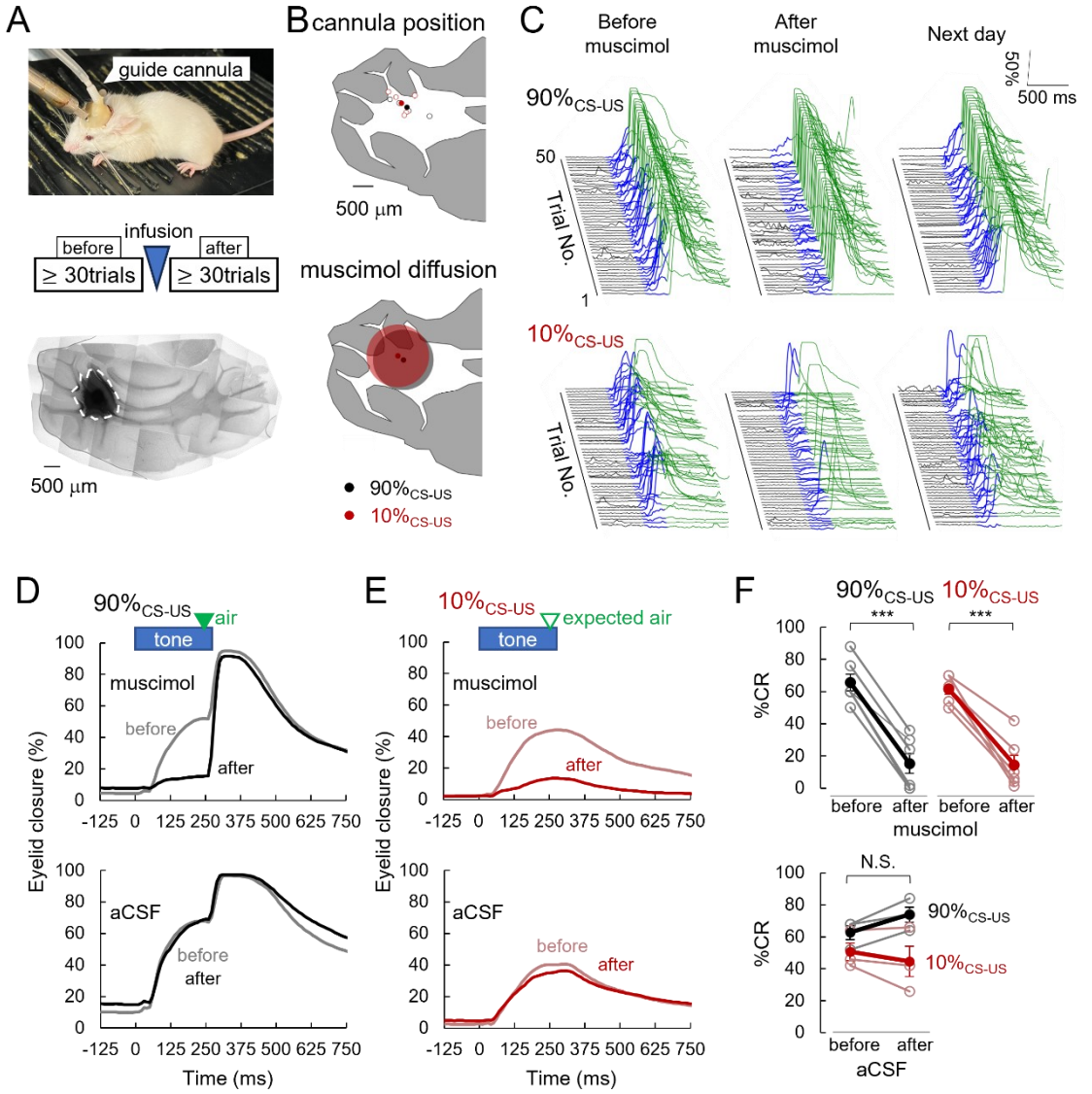

Fig 3. Critical role of DCN activity for occurrence of established CRs

(A, **B)** Schematics of pharmacological inactivation by muscimol (A) and the target location (B) in the cerebellum. Muscimol or aCSF was infused through an implanted guide cannula (top). Mice had at least 30 trials before/after muscimol or aCSF infusion (middle). Area for muscimol diffusion identified from fluorescence on a horizontal cryosection is shown in A, bottom (white dashed line), and summarized in B (90%$_{CS\text{-}US}$, n = 5; 10%$_{CS\text{-}US}$, n = 5). Cannula tip positions are also shown in B, top (90%$_{CS\text{-}US}$, n = 4; 10%$_{CS\text{-}US}$, n = 5). The distance of each average cannula position was less than 150 μm and the diameter of muscimol diffused area was 1.45 ± 0.19 mm for 90%$_{CS\text{-}US}$; 1.50 ± 0.12 mm for 10%$_{CS\text{-}US}$. (**C**) Representative eyelid traces from a single mouse in 90%$_{CS\text{-}US}$ (top) and 10%$_{CS\text{-}US}$ (bottom) before, after and the next day of muscimol infusion. (**D**, **E**) Averaged eyelid traces before/after muscimol (top) or aCSF (bottom) infusion in 90%$_{CS\text{-}US}$ (D,

836 n = 6) and $10\%_{CS\text{-}US}$ (E, n = 6). Eyelid traces from all acceptable trials were used for averaging.
837 (**F**) %CR changes before/after infusion of muscimol (top) and aCSF (bottom). ***, $p < 0.001$ by
838 paired t-test.

839

840

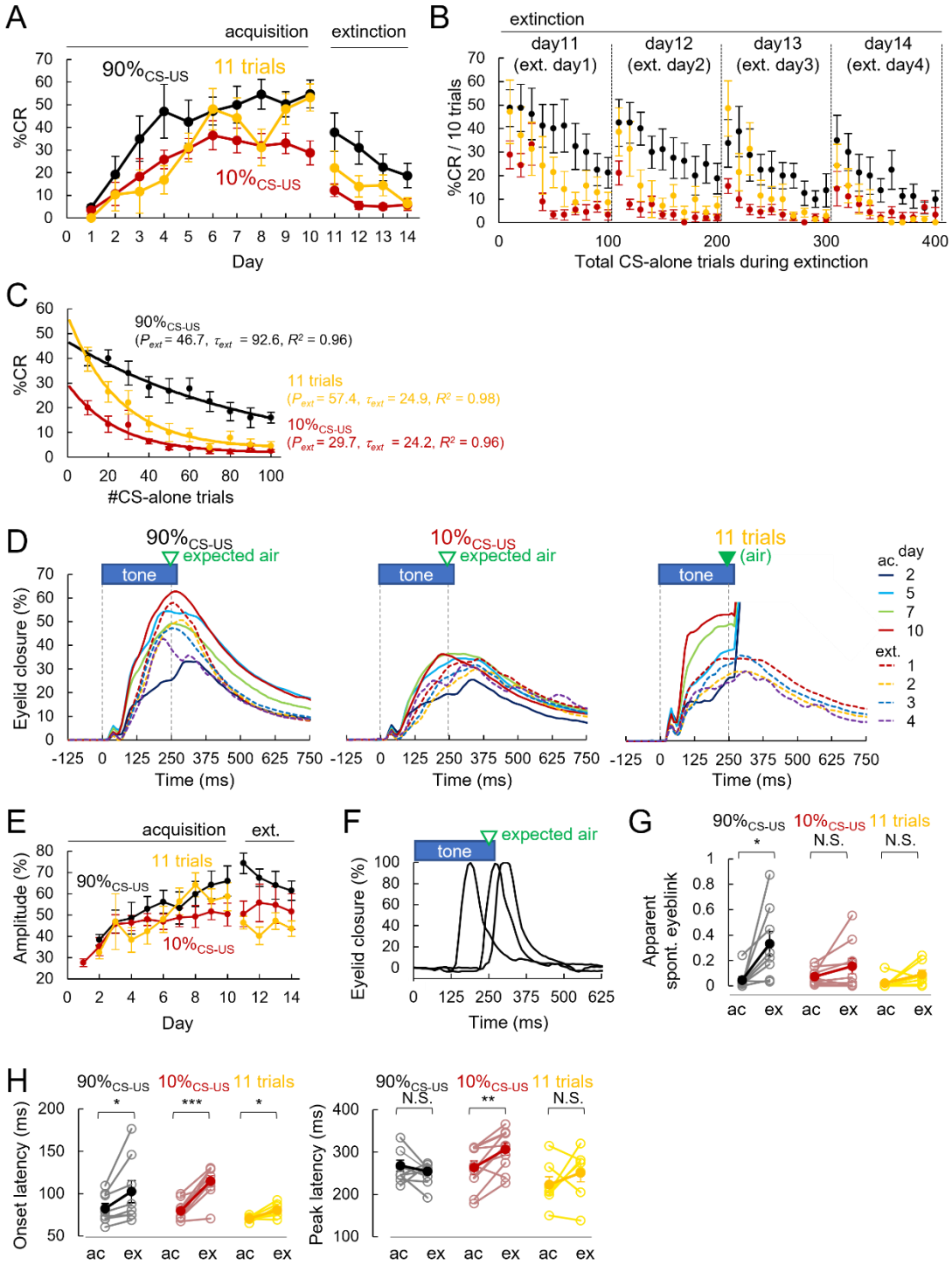

Fig 4. Dynamics of CR probability and eyelid closures during memory extinction

(A, **B**) Daily %CR changes during 14 days of training consisting of acquisition and extinction sessions (A) and %CR averaged from each 10 trial during 4 days extinction (B). 90%$_{CS\text{-}US}$, n = 8; 10%$_{CS\text{-}US}$, n = 9; 11 trials, n = 7. (**C**) Averaged %CR changes of every 10 trials from the beginning of extinction day1-4 were plotted against the number of CS-alone trials with fitting to single exponential curves. (**D**, **E**) Averaged eyelid closure traces on acquisition day2, 5, 7, 10 and

847 extinction day1-4 (D), indicated by different colors, and daily changes of averaged amplitude of
848 eyelid closure (E) during acquisition and extinction paradigms. For $90\%_{CS\text{-}US}$ and $10\%_{CS\text{-}US}$, from
849 CS-alone trials; for 11 trials, from both paired & CS-alone trials. The baseline level before CS
850 was aligned to 0% for each. (**F**) Example eyelid traces for responses like spontaneous eyeblink (>
851 90% of eyelid closure with half-width < 150 ms). (**G**) Ratio of spontaneous eyeblink-like ones to
852 all responses. Acquisition, ac; extinction, ex. *, $p < 0.05$ by paired t-test. (**H**) Onset latency (left)
853 and peak latency (right) during acquisition and extinction training. *, $p < 0.05$; **, $p < 0.01$; ***,
854 $p < 0.001$ by paired t-test.

855

856

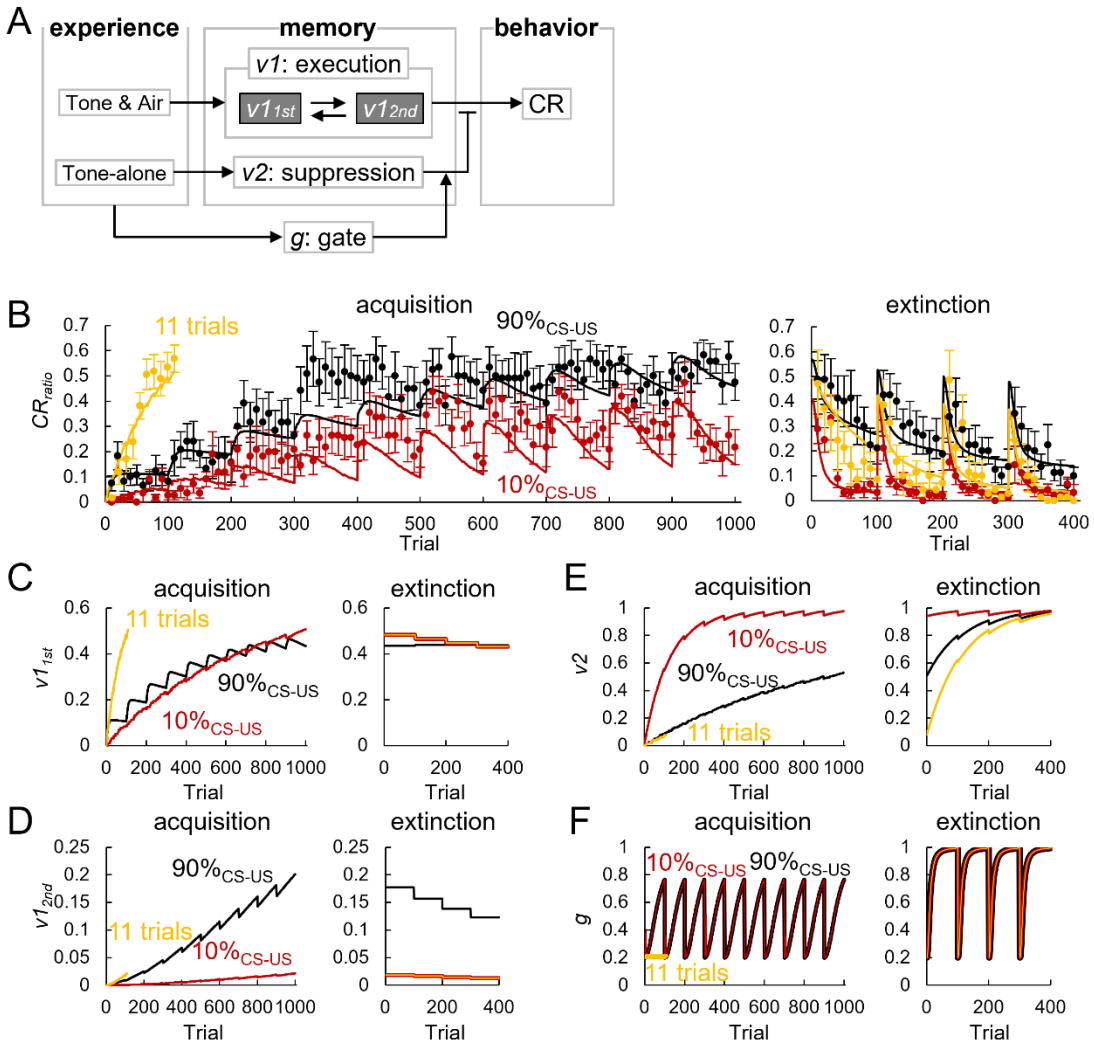

857 **Fig 5. Modeling of formation of counteracting memories for CRs**

858 **(A)** Model scheme for input-dependent memory formation for CR execution and its suppression.
859 **(B)** Simulated CR_{ratio} plotted as lines against total trial number during acquisition (left) and
860 extinction (right) paradigms, together with %CR averaged from each 10 or 11 trial recorded in
861 experiments (dots, 90%$_{CS\text{-}US}$, n = 12; 10%$_{CS\text{-}US}$, n = 11; 11 trials, n = 16). **(C-F)** Two components
862 for memory to execute CR, $v1_{1st}$ (C) and $v1_{2nd}$ (D), the counteracting memory to suppress CR, *v2*
863 (E), and its gate *g* (F) are plotted against total trial number during acquisition (left) and extinction
864 (right) in simulation.

865

866

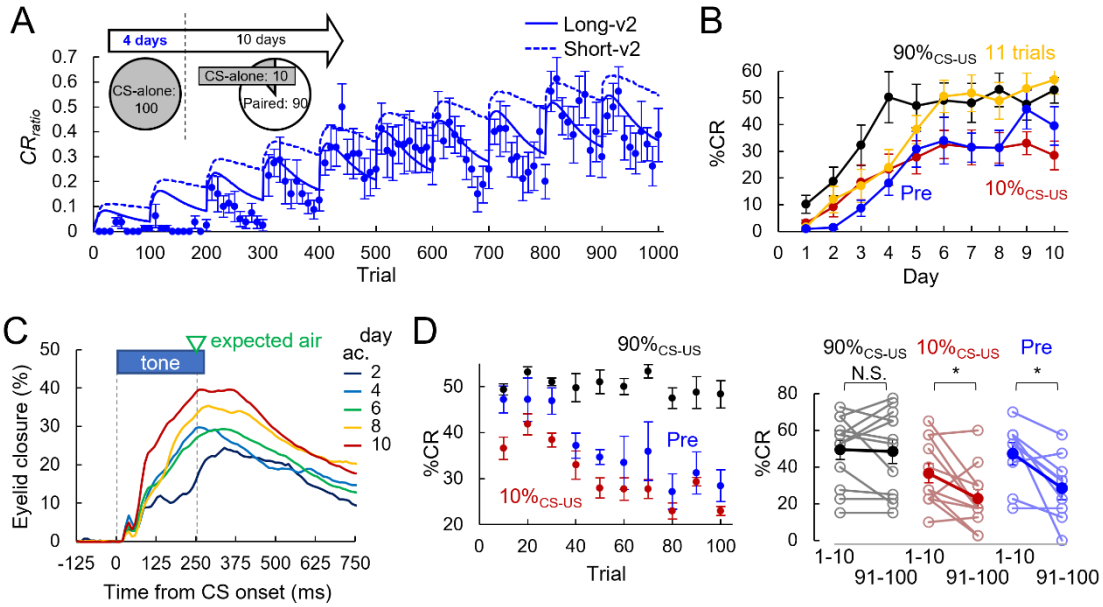

867 **Fig 6. Prediction and validation of long- or short-lasting suppression memory model**
868 (**A**) Prediction of CR_{ratio} changes during acquisition by 90%$_{CS\text{-}US}$ following the 4 days CS-alone
869 exposure (Pre) in models assuming long (solid line)- or short (dotted line)-lasting *v2*. Actual
870 experimental results of CR ratio averaged from each 10 trial (n = 8, dot) are also shown to
871 evaluate the model prediction. Training protocols for the Pre group is also shown as inset. **(B)**
872 Daily %CR changes during 10 days of acquisition training. Pre, n = 8. Data for the 90%$_{CS\text{-}US}$ (n
873 = 12), 10%$_{CS\text{-}US}$ (n = 11), and 11 trials (n = 16) shown in Fig. 1F are also superimposed for
874 comparison. **(C)** Averaged eyelid closures observed in CS-alone trials on day2, 4, 6, 8, 10 in the
875 Pre group mice which were given CS-alone trials for 4 days in prior to the 90% CS-US pairing.
876 (**D**) Averaged %CR for every 10 trials on day7-10 were plotted against trials number (left).
877 Comparison of averaged %CR in 1-10 and 91-100 trials (right). *, $p < 0.05$ by paired t-test.
878